HIF-1α Promotes Inflammatory Responses in *Aspergillus Fumigatus* Keratitis by Activating Pyroptosis Through Caspase-8/GSDMD Pathway

Hua Yang,[1] Mengzhu Liu,[1] Shiqi Song,[1] Qiang Xu,[1] Jieun Lee,[2] Jintao Sun,[1] Shasha Xue,[1] Xiaoyan Sun,[1] and Chengye Che[1]

[1]Department of Ophthalmology, the Affiliated Hospital of Qingdao University, Qingdao, China
[2]Department of Ophthalmology, School of Medicine, Pusan National University, Yangsan, Korea

Correspondence: Chengye Che, Department of Ophthalmology, The Affiliated Hospital of Qingdao University, 16 Jiangsu Rd., Qingdao 266003, China; chechengye@126.com.

HY, ML, and SS contributed equally to this work.

Received: October 13, 2024
Accepted: May 13, 2025
Published: June 10, 2025

Citation: Yang H, Liu M, Song S, et al. HIF-1α promotes inflammatory responses in *Aspergillus fumigatus* keratitis by activating pyroptosis through Caspase-8/GSDMD pathway. *Invest Ophthalmol Vis Sci.* 2025;66(6):32. https://doi.org/10.1167/iovs.66.6.32

Purpose. This research was designed to explore the expression patterns and functional significance of hypoxia-inducible factor-1α (HIF-1α) in the inflammatory response associated with *Aspergillus fumigatus* (*A. fumigatus*) keratitis.

Methods. Mouse models of *A. fumigatus* keratitis were created by scraping the corneal epithelium and applying *A. fumigatus* on the corneal surface. In the in vitro experiments, human corneal epithelial cells (HCECs) and THP-1 macrophages stimulated by *A. fumigatus* were used to investigate the cellular responses. HIF-1α was inhibited using LW6. Western blot, immunofluorescence, and quantitative reverse transcription polymerase chain reaction (qRT-PCR) were performed to assess the expression levels of HIF-1α in *A. fumigatus* keratitis. The inflammatory response was evaluated using clinical scoring, corneal thickness measurements, hematoxylin and eosin (H&E) staining, corneal fluorescein sodium staining, and a cell scratch test. The polarization of macrophages was determined using flow cytometry. The molecular mechanisms of HIF-1α were assessed by qRT-PCR and Western blot.

Results. In *A. fumigatus* keratitis, the expression of HIF-1α was significantly increased at both the mRNA and protein levels. Compared with the controls, HIF-1α inhibitor accelerated corneal epithelial repair, reduced the infiltration of macrophages, induced shift in macrophage polarization, and attenuated the inflammatory response. HIF-1α exerts a pro-inflammatory effect in *A. fumigatus* keratitis by modulating the expression of inflammatory mediators and engaging in pyroptosis via the caspase-8/GSDMD signaling pathway.

Conclusions. In conclusion, HIF-1α promotes *A. fumigatus* keratitis by inhibiting corneal epithelial repair and promoting inflammation, leading to increased severity of the disease.

Keywords: fungal keratitis (FK), HIF-1α, pyroptosis, inflammatory

Fungal keratitis (FK) is a major cause of monocular blindness, with *Aspergillus fumigatus* (*A. fumigatus*) being a significant pathogen.[1,2] FK has a poorer prognosis than bacterial keratitis due to limited treatment response and scarce antifungal medications.[3,4] Thus, identifying new pathogenic pathways and therapeutic targets for FK is critical.

One of the most important functions of the cornea is maintaining homeostasis.[5,6] FK often occurs with epithelial damage, disruption of the corneal barrier function, and pathogen invasion into the corneal tissue, triggering infection. The corneal epithelium frequently detects pathogen-associated molecular patterns (PAMPs) during infection, such as the "non-self" structure of fungi. These PAMPs activate pattern recognition receptors (PRRs) and subsequently initiate an immune response, promoting the recruitment of macrophages and neutrophils.[7,8] Activation of these receptors triggers immune and inflammatory responses to combat infection, repair tissue damage, and restore homeostasis.[9,10]

The molecular details of the complex process of pathogen infection and corneal tissue regeneration are still being uncovered. Recent research has started to reveal how tissue injury triggers acute inflammatory responses.[11–14] Hypoxia-inducible factor-1α (HIF-1α) serves as a transcription factor that modulates the activation of immune cells, angiogenesis, cell proliferation or survival, and glucose and iron metabolism.[15,16] As a result, HIF-1α plays a role in various conditions that create hypoxic microenvironments, including cancer, stroke, and heart disease.[17–19] However, it remains largely unclear if and how HIF-1α contributes to corneal tissue damage and initiates the innate immune response to infection.

In the current study, we developed both mouse and cellular models of *A. fumigatus* infection to examine the

potential involvement of HIF-1α in the inflammatory response and tissue repair processes.

Methods

Mice

Female wild-type C57BL/6 mice, aged 6 to 8 weeks, were obtained from Jinan Pengyue Laboratory Animal Co., Ltd., Jinan, China (vendor license number: SCXK [Lu] 2022–0006). The study protocol was approved by the Animal Care and Use Committee of the Affiliated Hospital of Qingdao University and adhered to the Association for Research in Vision and Ophthalmology (ARVO) Statement on the Use of Animals in Ophthalmic and Vision Research.

Mouse Model of *A. Fumigatus* Keratitis

The mouse model was established according to a previously published protocol.[20] Mice were anesthetized via intraperitoneal injection with a mixture of ketamine (100 mg/kg) and xylazine (15 mg/kg). A sterile 26-gauge needle was used to gently scrape the central corneal epithelium of the right eye, creating 2-mm-diameter incisions to disrupt the epithelial barrier. After applying *A. fumigatus* (1×10^8 colony-forming units [CFU]/mL) topically to the injured cornea, a soft contact lens was applied, followed by suturing of the eyelids for 24 hours.

Cell Culture

Human corneal epithelial cells (HCECs) were procured from the Ocular Surface Laboratory of the Zhongshan Ophthalmic Center. The cells were cultured in an equal mixture of Dulbecco's Modified Eagle Medium (DMEM) and Ham's F12, fortified with 5% fetal bovine serum and 1% penicillin-streptomycin. THP-1 macrophages were sourced from Meilunbio in Dalian, China, and differentiated using phorbol-12-myristate 13-acetate (PMA) at a concentration of 100 ng/mL for 24 to 48 hours. These macrophages were cultured in RPMI-1640 medium.

Administration of HIF-1α Inhibitor

LW6, used as a HIF-1α inhibitor in this study, was purchased from MedChemExpress (MCE, USA, 13671). The mice received 2 subconjunctival injections of LW6 (100 µM) over 1 day, with PBS serving as the control. Two hours after the second subconjunctival injection, the corneas were infected with *A. fumigatus*. LW6 (10 µM) was administered to THP-1 macrophages and HCECs for a duration of 2 hours prior to stimulation with *A. fumigatus* spores.

Clinical Examination and Corneal Thickness Measurement

Clinical scores were assigned using Wu et al.'s scoring system by two independent observers in a blinded manner.[21] A detailed description of the scoring criteria is within Table 1. Corneal thickness was assessed using anterior segment optical coherence tomography, with the TOPI-SIGMA-1000 device (TowardPi, China).

Quantification of Colony-Forming Units

To determine the fungal growth in the cornea, the entire mouse corneas were processed under aseptic conditions. The samples were homogenized in 1 mL of PBS using the Mixer Scientz-48 (Scientz, Ningbo, China) at a frequency of 33 hertz (Hz) for 4 minutes. Following homogenization, serial dilutions were prepared and plated onto Sabouraud dextrose agar plates (BDMS, Cockeysville, MD, USA). The inoculated plates were subsequently incubated at 37°C for 24 hours, after which the CFUs were quantified by direct counting.

CCK-8 Cell Activity Assay

The activity of THP-1 macrophages was assessed using the CCK-8 method. The cells were subjected to a 2-hour pretreatment with PBS or LW6 and stimulated with hyphae for 24 hours. Each well was then supplemented with 100 µL of serum-free medium (SFM) and 10 µL of CCK-8 solution (Meilunbio, Dalian, China). Following an incubation period of 2.5 hours at 37°C, the absorbance was measured at a wavelength of 450 nm using a microplate reader.

LDH Release Assay

The LDH release assay was conducted to evaluate cell membrane integrity. THP-1 macrophages were pretreated and stimulated same with CCK-8 assay. Following the instructions of the LDH Cytotoxicity Assay Kit (MCE, USA), the appropriate reagents were added, and the absorbance was measured at a wavelength of 490 nm.

Corneal Fluorescein Sodium Staining

The extent of corneal epithelial defects was assessed using corneal fluorescein sodium staining. Ninety percent of the corneal epithelium was gently scraped using a blade. Corneal fluorescein sodium staining was performed at 0, 8, 16, and 24 hours following epithelial damage using slit-lamp microscopy equipped with a cobalt blue light.

Table 1. Clinical Scoring System

Score	Corneal Opacity Area	Corneal Opacity Density	Corneal Surface Regularity
1	1%–25%	Slight cloudiness (outline of iris and pupil discernable)	Slight surface irregularity
2	26%–50%	Cloudy (but outline of iris and pupil remain visible)	Rough surface (some swelling)
3	51%–75%	Cloudy (opacity not uniform)	Significant swelling (crater or serious descemetocele formation)
4	76%–100%	Uniform opacity	Perforation or descemetocele

Total score is the sum of opacity area, density, and surface regularity scores.

Investigative Ophthalmology & Visual Science

Table 2. Primer Sequences Used for qRT-PCR

Gene	Primer Sequence (5′-3′)
Mouse β-actin	F: CATCCGTAAAGACCTCTATGCCAAC; R: ATGGAGCCACCGATCCACA
Mouse HIF-1α	F: GAAACGACCACTGCTAAGGCA; R: GGCAGACAGGTTAAGGCTCCT
Mouse TNF-α	F: ACCCTACACTCAGATCATCTT; R: GGTTGTCTTTGAGATCCATGC
Mouse IL-6	F: CACAAGTCCGGAGAGGAGAC; R: CAGAATTGCCATTGCACAAC
Mouse IL-10	F: TGCTAACCGACTCCTTAATGCAGGAC; R: CCTTGATTTCTGGGCCATGCTTCTC
Mouse IL-1β	F: CGCAGCAGCACATCAACAAGAGC; R: TGTCCTCATCCTGGAAGGTCCACG
Human GAPDH	F: GCACCGTCAAGGCTGAGAAC; R: TGGTGAAGACGCCAGTGGA
Human HIF-1α	F: AGAGGTTGGGGGAGGAGAGAT; R: GCACCAGCAGGTCATAGGT
Human TNF-α	F: ACCCTCACACTCAGATCATCTT R: GGTTGTCTTTGAGATCCATGC
Human IL-6	F: AAGCCAGAGCTGTGCAGATGAGTA; R: TGTCCTGCAGCCACTGGTTC
Human IL-10	F: GACTTTAAGGGTTACCTGGGTTG R: TCACATGCGCCTTGATGTCTG
Human IL-1β	F: ATGCACCTGTACGATCACTGA; R: ACAAAGGACATGGAGAACACC

F, forward; R, reverse.

Table 3. Antibodies Used for Western Blot, Immunofluorescence, and Flow Cytometry

Antibody	Company	Order Number	Remarks
HIF-1α	Cell Signaling Technology, America	36169S	Western blot
TNF-alpha	Proteintech, China	17590-1-AP	Western blot
IL-6	Proteintech, China	21865-1-AP	Western blot
IL-10	Proteintech, China	60269-1-Ig	Western blot
caspase-1	Proteintech, China	22915-1-AP	Western blot
caspase-8	Proteintech, China	13423-1-AP	Western blot
GSDMD	Novus, America	NBP2-33422	Western blot
IL-1 beta	R&D Systems, America	AF-401-NA	Western blot
β-actin	Cell Signaling Technology, America	4967	Western blot
F4/80	Santa Cruz Biotechnology, America	sc-377009	Immunofluorescence
Anti-rabbit IgG 488 Conjugate	Cell Signaling Technology, America	4408	Immunofluorescence
Anti-rabbit IgG 555 Conjugate	Cell Signaling Technology, America	4413	Immunofluorescence
PE/Cyanine7 anti-mouse CD45	BioLegend, America	103114	Flow cytometry
FITC anti-mouse F4/80	BioLegend, America	123108	Flow cytometry
APC anti-mouse CD86	BioLegend, America	105012	Flow cytometry
PE anti-mouse CD206(MMR)	BioLegend, America	141705	Flow cytometry

Cell Scratching Assay

HCECs were seeded and grown until the cell density exceeded about 90%. Four parallel lines were drawn at the bottom of the wells using a sterile pipette tip. The cells were then cultured in media containing either PBS or LW6. Scratch width was recorded at 0, 24, and 48 hours under a light microscope to assess cell migration ability.

Hematoxylin and Eosin Staining

Mouse eyeballs were immersed in 4% paraformaldehyde solution for 3 days, followed by sectioning into 8-µm thick slices. Paraffin embedding was carried out, and the sections were hydrated using an ethanol gradient after dewaxing in xylene. Hematoxylin and eosin (H&E) staining was performed, and the sections were examined under the light microscope.

Quantitative Real-Time Polymerase Chain Reaction

Total RNA was isolated from the samples using the RNAiso Plus kit (Takara, Dalian, China). Subsequently, the extracted RNA was reverse-transcribed into complementary DNA (cDNA) using the PrimeScript RT kit (Takara, Dalian, China). The cDNA was then amplified via quantitative real-time PCR using the SYBR Green PCR Master Mix (Vazyme, China) on an Eppendorf Mastercycler system. GAPDH or β-actin was used as the internal reference gene. The relative expression levels were calculated using the $\Delta\Delta$CT method. The primers used in this study are detailed in Table 2.

Western Blot

Cells and mouse cornea samples were lysed using RIPA buffer. The protein samples were separated by 10%–12% sodium dodecyl sulfate-polyacrylamide gel electrophoresis (SDS-PAGE) and transferred onto Millipore polyvinylidene difluoride (PVDF) membranes. The membranes were blocked with 3% BSA blocking buffer (Beyotime, Shanghai, China) for 2 hours, then incubated with primary antibodies overnight at 4°C and secondary antibodies for 2 hours. Chemiluminescent signals were detected using a Vilber Fusion FX imaging system. The antibodies used in this study are listed in Table 3.

Immunofluorescence Staining

Mouse eyeball sections (8 µm) and cell slides were immersed in paraformaldehyde for 30 minutes and blocked with 10% animal serum (Solarbio, Beijing, China). Sections were incubated with primary antibodies at 4°C overnight and secondary antibodies for 1 hour. Nuclei were stained with

Investigative Ophthalmology & Visual Science

DAPI solution (Solarbio, China) for 10 minutes. Images were acquired using the EVOS M5000 microscope. The antibodies utilized in this study are detailed in Table 3.

Flow Cytometry

The excised corneas underwent treatment with 50 µL of Liberase TL (2.5 mg/mL, 5401020001; Roche, Basel, Switzerland) for 40 minutes at a temperature of 37°C. They were then homogenized via a 70-µm cell strainer to prepare single-cell suspensions. We referenced the gating strategy for macrophage polarization used in previous flow cytometry experiments.[22,23] Flow cytometry was used to analyze the single-cell suspensions of the cornea using a CytoFLEX S instrument (Beckman Coulter, USA) and analyzed using FlowJo version 10.8.1 software. Details regarding the antibodies utilized are presented in Table 3.

Statistical Analysis

Statistical analyses were conducted using GraphPad Prism 10 software. For comparisons between the 2 groups, an unpaired 2-tailed *t*-test was used, whereas -way analysis of variance (ANOVA) was used for comparisons involving more than 2 groups.

Results

A. Fumigatus Infection Induced HIF-1α Expression in Mouse Corneas

To verify the effects of *A. fumigatus* infection in mouse corneas, we photographed the corneas at 1, 3, and 5 dpi. As shown in Figure 1A, corneal opacity increased following infection, and clinical scores are displayed in the accompanying chart. Compared with naïve corneas, HIF-1α mRNA and

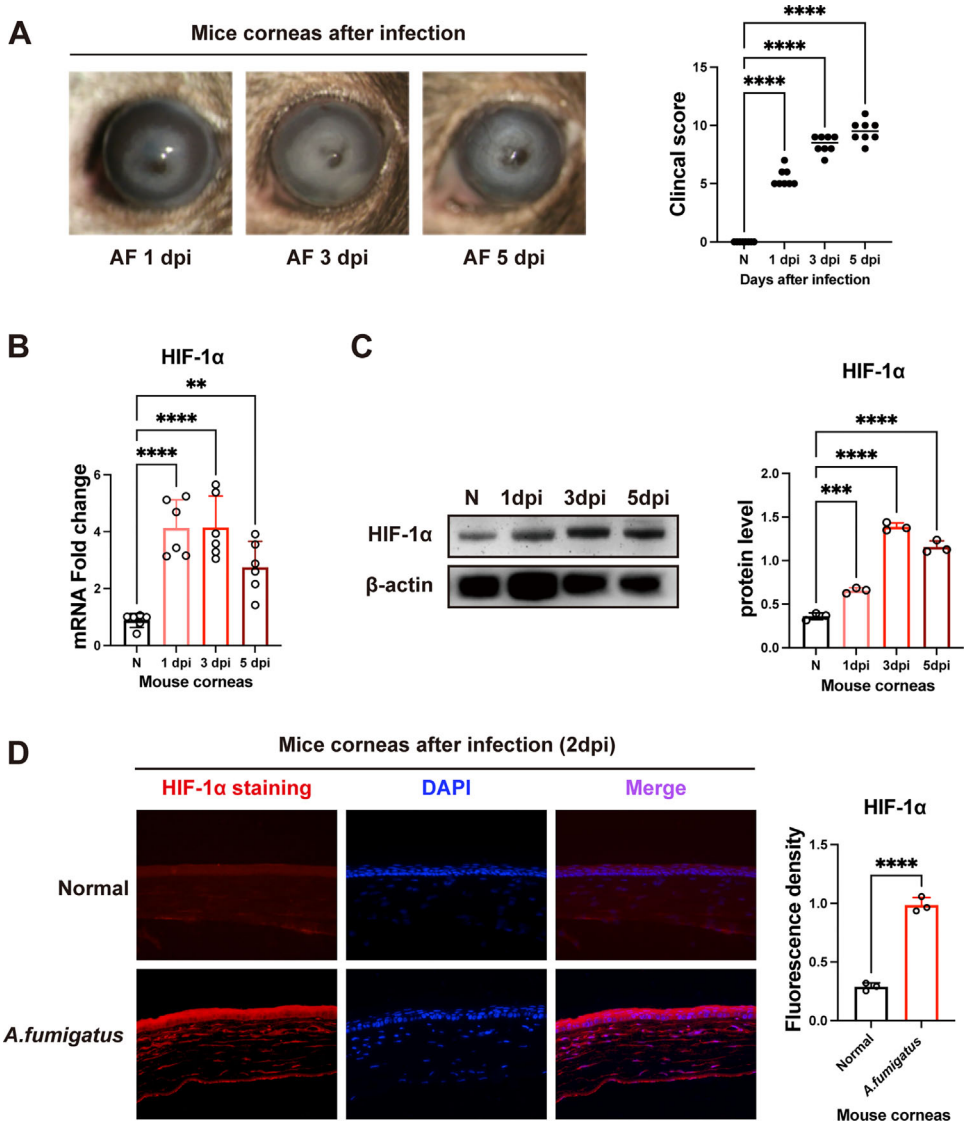

Figure 1. *A. fumigatus* infection induces HIF-1α expression in C57BL/6 mouse corneas. (**A**) Slit-lamp images of mouse corneas with *A. fumigatus* keratitis at 1, 3, and 5 dpi, with clinical scores shown in the accompanying statistical chart. (**B**) The qRT-PCR of HIF-1α mRNA expression in naïve and *A. fumigatus* infected corneas. (**C**) Western blot analysis of HIF-1α protein in corneas from *A. fumigatus* keratitis groups compared to the naïve group at 1, 3, and 5 dpi. (**D**) IF staining of HIF-1α at 2 dpi (40 × magnification). The stars at the top of each column represent *P* values comparing to the normal control. ns, non-significant, $^{**}P < 0.01$, $^{***}P < 0.001$, $^{****}P < 0.0001$ (ANOVA). Data are presented as mean ± SEM from three independent experiments.

Investigative Ophthalmology & Visual Science

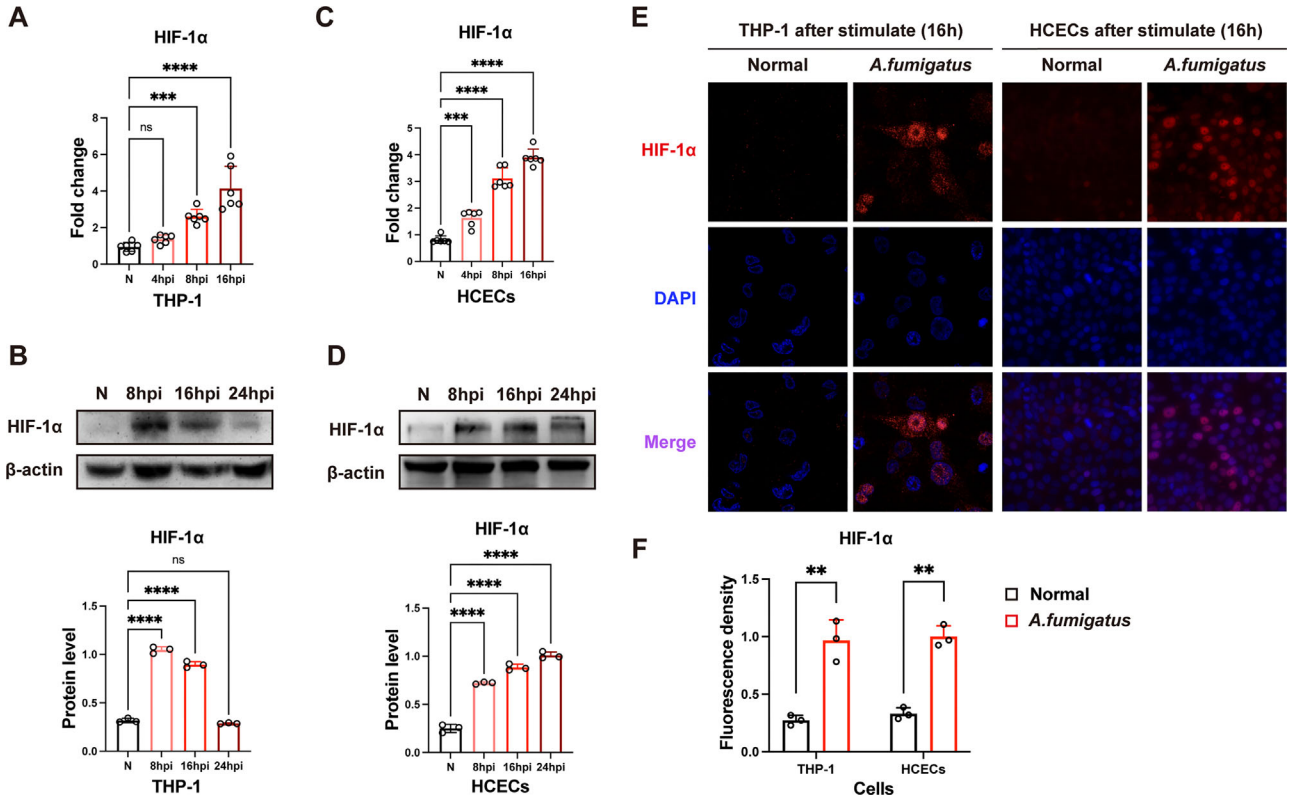

Figure 2. *A. fumigatus* stimulation induces HIF-1α expression in THP-1 macrophages and HCECs. The qRT-PCR of HIF-1α in THP-1 macrophages (**A**) and HCECs (**C**) were performed at 4, 8, and 16 hpi. Western blot analysis of HIF-1α protein expression in THP-1 macrophages (**B**) and HCECs (**D**) was performed at 8, 16, and 24 hpi, with quantification shown in bar graphs. (**E**) IF staining of HIF-1α in THP-1 macrophages and HCECs was performed at 16 hpi (40 × magnification). (**F**) Shows the statistical analysis of fluorescence density in Figure **E**. The *stars* at the top of each column represent *P* values comparing to the normal control. ns, nonsignificant, ***$P < 0.001$, ****$P < 0.0001$ (ANOVA). Data are presented as mean ± SEM from three independent experiments.

protein levels were elevated from 1 to 5 dpi (Figs. 1B, 1C). To identify the source of HIF-1α in the cornea, samples were collected on 2 dpi for immunofluorescence (IF) experiments. Figure 1D shows that HIF-1α was primarily localized in the infected corneal epithelium and stromal layer.

A. Fumigatus Stimulation Increased HIF-1α Expression in THP-1 Macrophages and HCECs

HIF-1α mRNA expression showed a progressive increase in THP-1 macrophages, peaking at 16 hours post-infection (hpi; Fig. 2A). At the protein level, HIF-1α expression was significantly elevated at 8 hpi, decreased by 16 hpi, and continued to decline (Fig. 2B). HIF-1α mRNA expression was first detected at 4 hpi and increased significantly by 16 hpi (Fig. 2C). HIF-1α protein expression rose at 8 hpi and decreased by 24 hpi (Fig. 2D). IF staining at 16 hpi revealed HIF-1α localization in the cytoplasm and nucleus of both THP-1 macrophages and HCECs (Fig. 2E).

Inhibiting HIF-1α Enhanced Corneal Epithelial Repair

HIF-1α, a transcription factor associated with injury,[24] may play a role in corneal epithelial repair. Western blotting of THP-1 macrophages and corneas confirmed effective inhibition of HIF-1α by LW6 (10 µM) in vitro, and downregulation of HIF-1α in vivo with LW6 (100 µM; Figs. 3A, 3B). As shown in Figure 3C, corneal epithelial repair was faster after HIF-1α inhibition compared to the PBS control. Similarly, HIF-1α inhibitor increased the migration of HCEC cells (Fig. 3D). These results demonstrate that inhibiting HIF-1α enhanced corneal epithelial repair.

Inhibiting HIF-1α Reduced the Severity of *A. Fumigatus* Keratitis in Mouse Corneas

The severity of FK was quantified using a clinical scoring system that assessed ulcer area, opacity density, and ulcer morphology.[21] At 2 dpi, the PBS control corneas exhibited severe keratitis, whereas the LW6-injected corneas showed less severe keratitis, thinner corneal thickness, and fewer inflammatory cells in the central corneas, as observed in H&E staining (Fig. 4A). Compared with PBS-treated controls, LW6-treated mouse corneas exhibited a higher fungal burden at 2 dpi (Fig. 4D). The IF staining demonstrated that macrophage infiltration in the corneal stroma was reduced following LW6 injection compared to the control group (Fig. 4E). The CCK8 results showed that after infection with *A. fumigatus*, cell viability decreased, whereas treatment with LW6 could rescue the reduced cell viability (Fig. 4G). Compared with the PBS-treated group stimulated by *A. fumigatus*, the LDH release was significantly reduced after treatment with LW6 (Fig. 4H). These research findings suggest that inhibiting HIF-1α may impair immune activation by affecting pyroptosis, leading to an increased fungal burden.

Investigative Ophthalmology & Visual Science

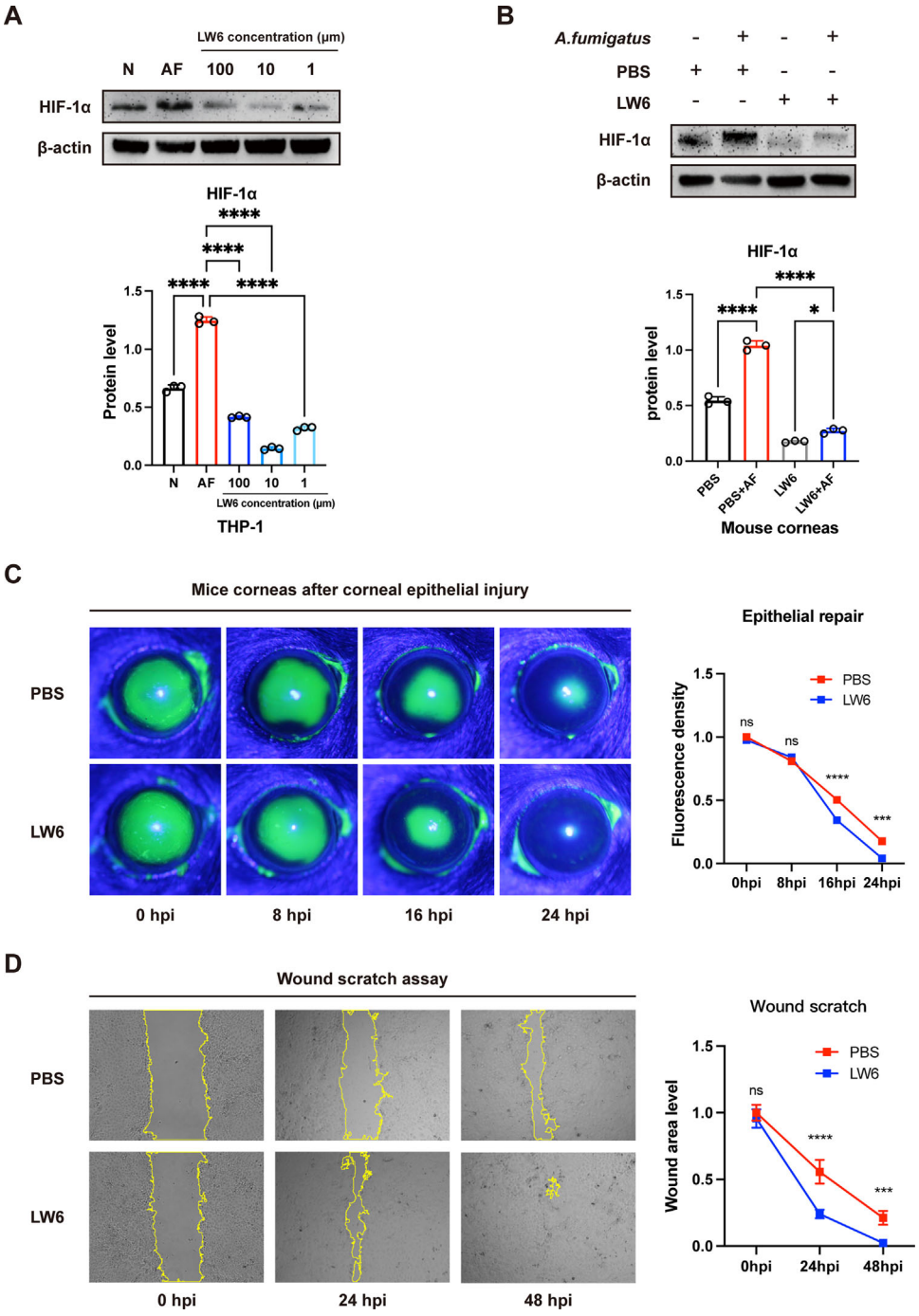

Figure 3. The repair capacity of the corneal epithelium increased following HIF-1α inhibition. (**A**) Immunoblot analysis of HIF-1α in THP-1 macrophage cell lysates treated with different concentrations of LW6 or PBS (control) at 16 hpi. (**B**) Mice were subconjunctivally injected with 100 μM LW6 or PBS, and corneas were collected at 2 dpi for Western blot analysis to detect HIF-1α expression. (**C**) Cobalt blue light images were captured at 0, 8, 16, and 24 hours after applying fluorescein sodium solution to the eyes. The *green fluorescence* indicates the area of corneal epithelial defects. Corneal epithelial healing rate is shown in the *broken line graph*. (**D**) The healing ability of HCECs was evaluated using a cell wound scratch assay. *Yellow lines* represent the cell edges. The wound healing rate is shown in the *broken line graph*. *P* values were calculated using 1-way ANOVA for panels **A** and **B**, and an unpaired Student's *t*-test for panels **C** and **D**. ns, nonsignificant, $^{***}P < 0.001$, $^{****}P < 0.0001$. Data are presented as mean ± SEM from three independent experiments, with six mice per group.

Inhibiting HIF-1α Affected the Macrophage Polarization

Macrophages derived from mouse corneas were analyzed using flow cytometry (Fig. 5A). On 2 dpi, compared with the PBS-treated group, the LW6-treated group showed a significant reduction in the total macrophages cell rate, M1 macrophage cell rate. Meanwhile, the ratio of M2 to M1 was elevated. Cytokines involved in macrophage polarization-related cytokines were also altered. As shown in Figure 5C,

Investigative Ophthalmology & Visual Science

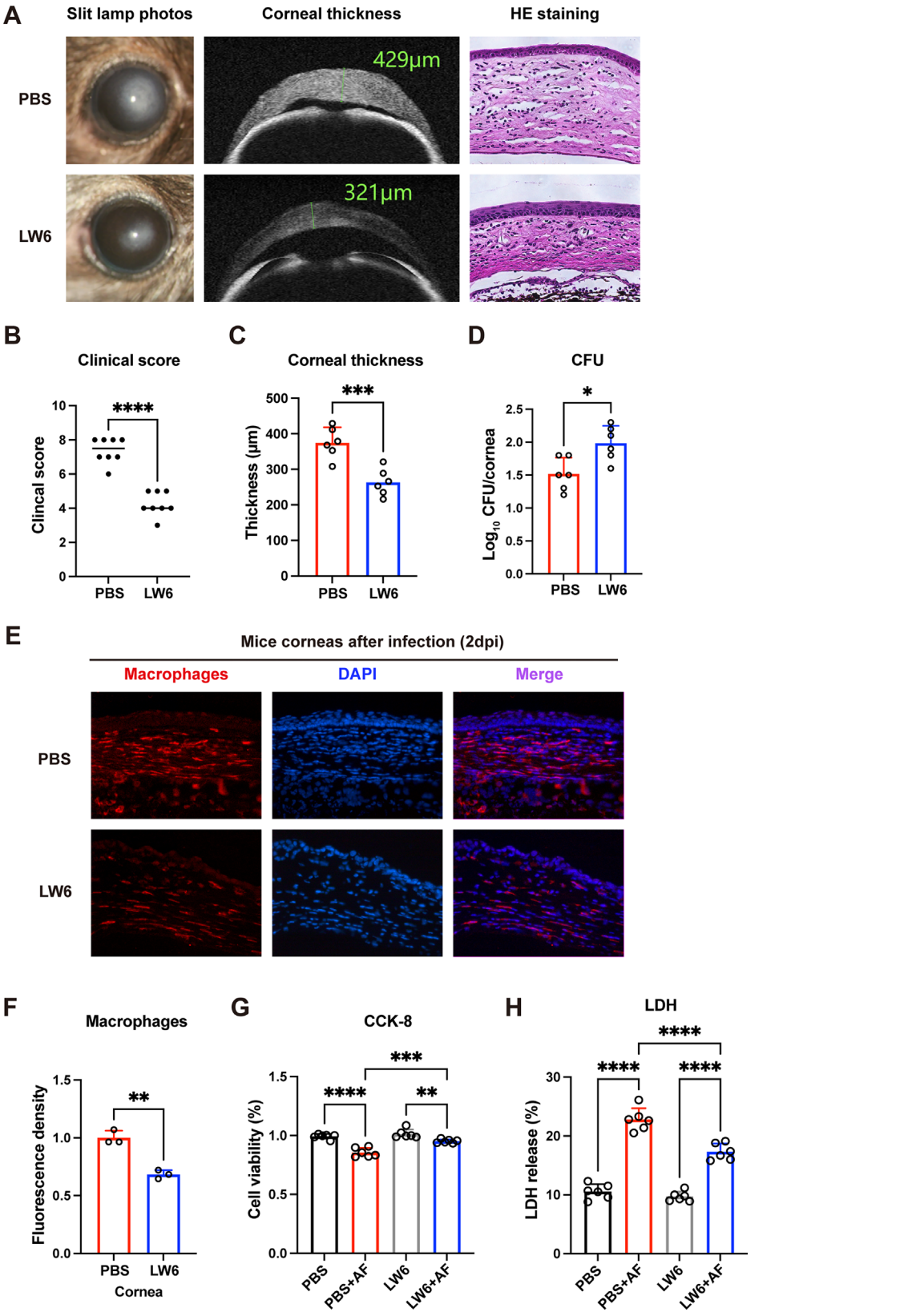

Figure 4. Inhibiting HIF-1α reduces the severity of *A. fumigatus* infection in mouse corneas. (**A**) Mouse corneas were monitored daily, and images were captured up to 2 dpi. Slit-lamp images were used to assess the clinical score, anterior segment optical coherence tomography was used to observe corneal edema, and H&E staining was performed to detect inflammatory cell infiltration in the central corneas. Clinical scores (**B**) and corneal thickness (**C**) were measured daily and statistically analyzed. (**D**) As shown by the CFUs, HIF-1α inhibitor led to higher fungal load at 2 dpi. (**E**) F4/80 *red fluorescence* indicates infiltrating macrophages in the cornea, (**F**) as observed through IF analysis. (**G**) The viability of THP-1 macrophages was assessed using a CCK-8 assay. (**H**) The integrity of THP-1 macrophage membranes following various treatments was evaluated via an LDH release assay. *$P < 0.05$, **$P < 0.01$, ***$P < 0.001$, ****$P < 0.0001$. Data are presented as mean $\pm$ SEM from three different experiments.

Investigative Ophthalmology & Visual Science

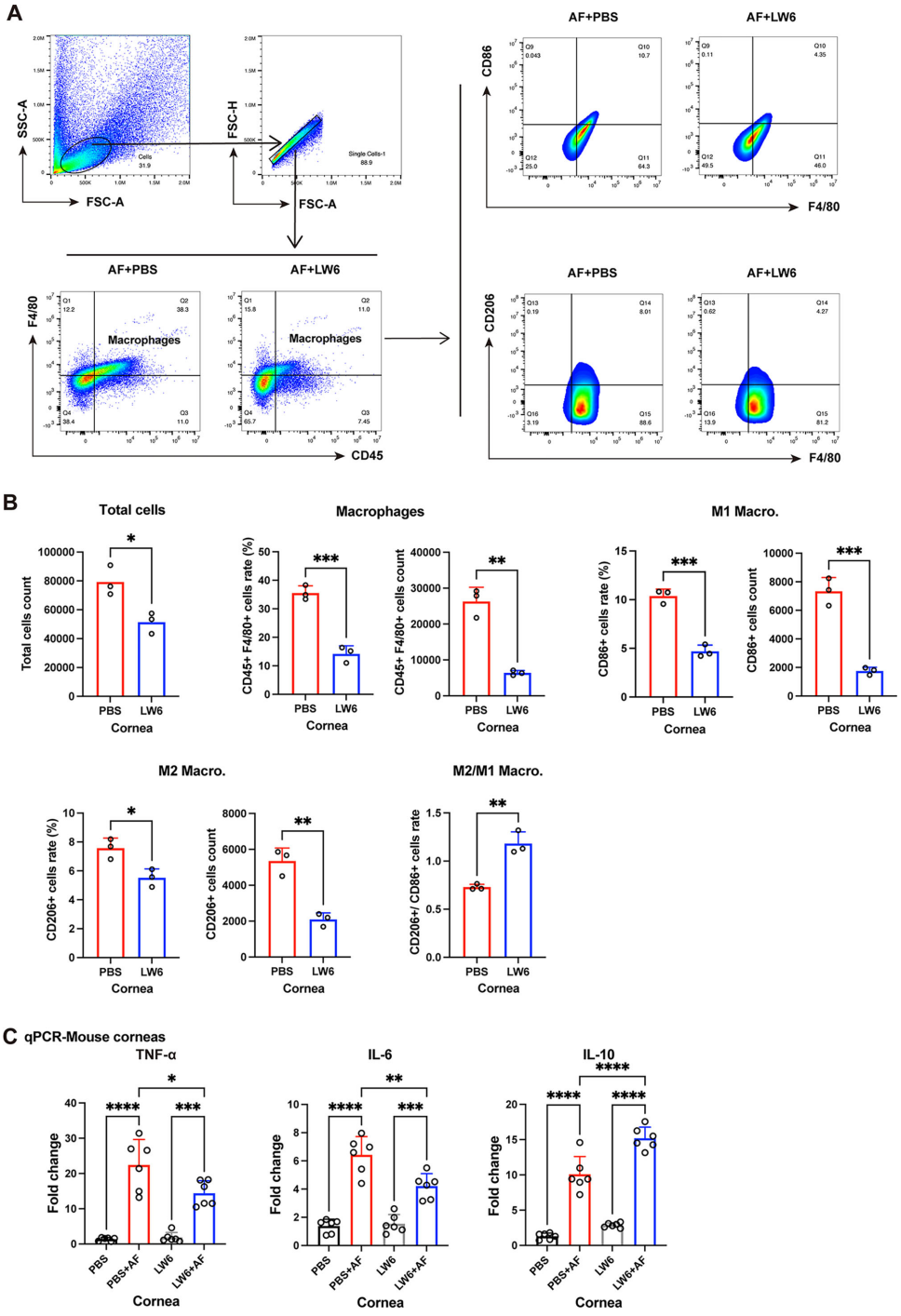

Figure 5. The influence of HIF-1α on the polarization of corneal macrophages and expression of TNF-α, IL-6, and IL-10 in mouse corneas and THP-1 macrophages. (**A**) The corneas of mice infected with *A. fumigatus* were collected after 2 dpi. Whole corneas treated with PBS or LW6 were subjected to flow cytometry analysis. On a single-cell level, CD45+ cells are indicative of immune cells. Specifically, CD45+F4/80+ cells are identified as macrophages. Within the macrophage population, CD86+ cells are classified as M1 macrophages, whereas CD206+ cells are categorized as M2 macrophages. (**B**) Representative dot plots show the numbers and percentages of total cells, macrophages, M1 macrophages, M2 macrophages, as well as the M2/M1 ratio. (**C**) The qRT-PCR were conducted to measure TNF-α, IL-6, and IL-10 mRNA in mouse corneas at 2 dpi. (**D**) The qRT-PCR was conducted in THP-1 macrophages at 8 hpi. (**E**) Western blot analyses were conducted to measure TNF-α, IL-6, and IL-10 protein levels in mouse corneas at 2 dpi. (**F**) In addition, the Western blot was conducted in THP-1 macrophages at 16 hpi. The *P* values were generated using 1-way ANOVA, with ns = nonsignificant, *$P < 0.05$, **$P < 0.01$, ***$P < 0.001$, and ****$P < 0.0001$. Data are presented as mean ± SEM from three different experiments with six mice per group.

Investigative Ophthalmology & Visual Science

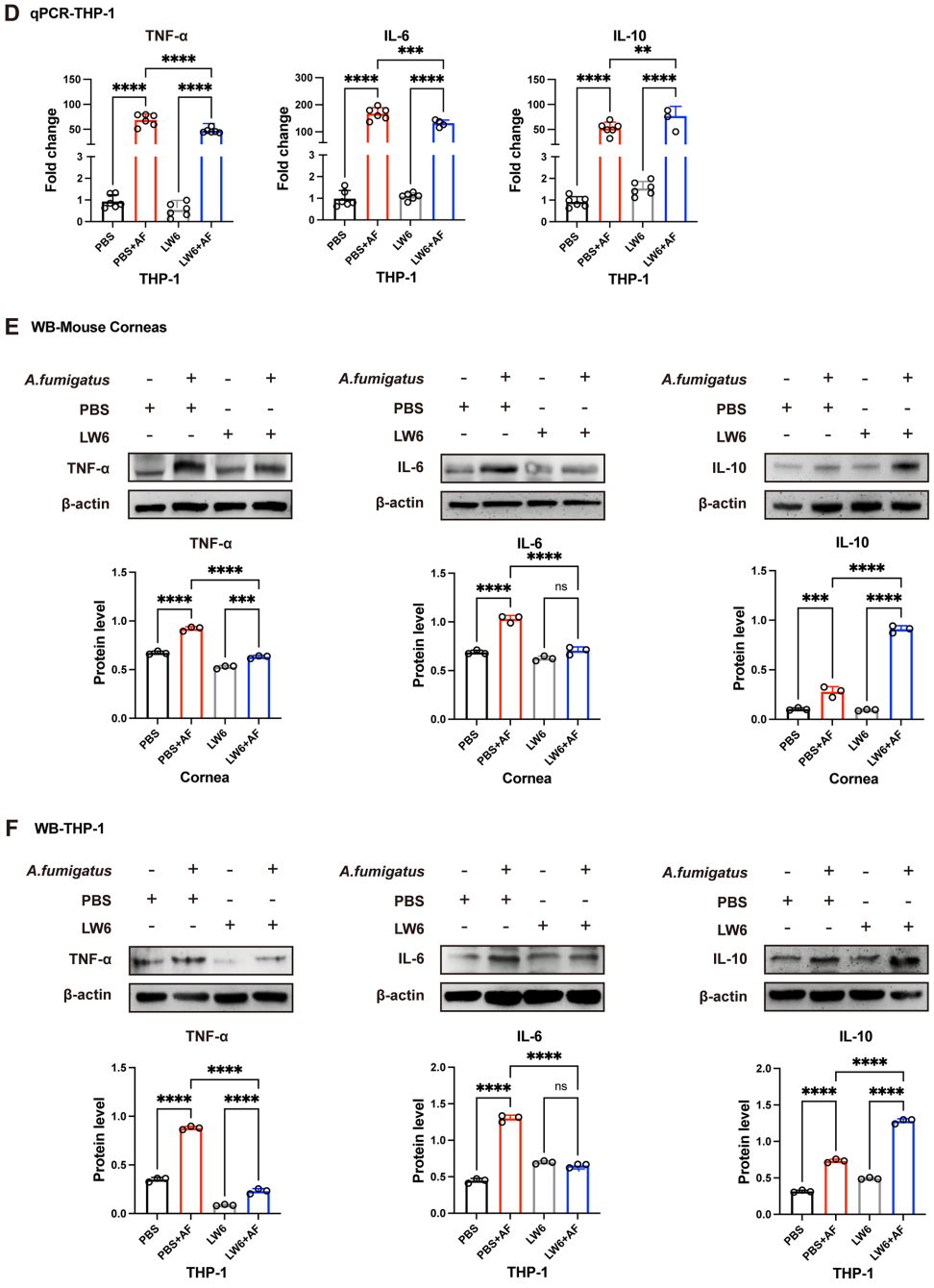

Figure 5. Continued.

A. fumigatus infection enhanced the expression of TNF-α and IL-6 at both the mRNA levels, whereas LW6 reduced their expression in the infected corneas. Notably, inhibiting of HIF-1α further increased IL-10 expression in the infected corneas. Consistent with the in vivo results, the expression of TNF-α, IL-6, and IL-10 was also induced by *A. fumigatus* infection in the in vitro study (Fig. 5D). This expression was further validated at the protein level (Figs. 5E, 5F).

HIF-1α Regulated the Caspase-8/GSDMD Pyroptosis Pathway, Contributing to the Inflammatory Response to *A. Fumigatus* Keratitis

Pyroptosis plays a critical regulatory role in FK.[25] Cell membrane rupture is an important characteristic of pyroptosis.[26] The results of the CCK8 and LDH assays (see Figs. 4H, 4I) suggest that HIF-1α mediates the occurrence of pyroptosis. Although caspase-1 involved in the pyroptosis classical pathway were unaffected by LW6, the active form, clv-caspase-8, N-terminal GSDMD (N-GSDMD), and the downstream factor interleukin-1 beta (IL-1β) exhibited marked upregulation following HIF-1α inhibitor in *A. fumigatus*-infected corneas (Fig. 6A). Consistent with the results observed in mouse corneas, the protein expression of clv-caspase-8, N-GSDMD, pro-IL-1β, and clv-IL-1β was induced by *A. fumigatus* stimulation and attenuated with HIF-1α inhibitor in THP-1 macrophages (Fig. 6C). Consequently, HIF-1α inhibitor resulted in the downregulation of the caspase-8/GSDMD pathway in *A. fumigatus*-infected corneas. The decreased host response and significantly

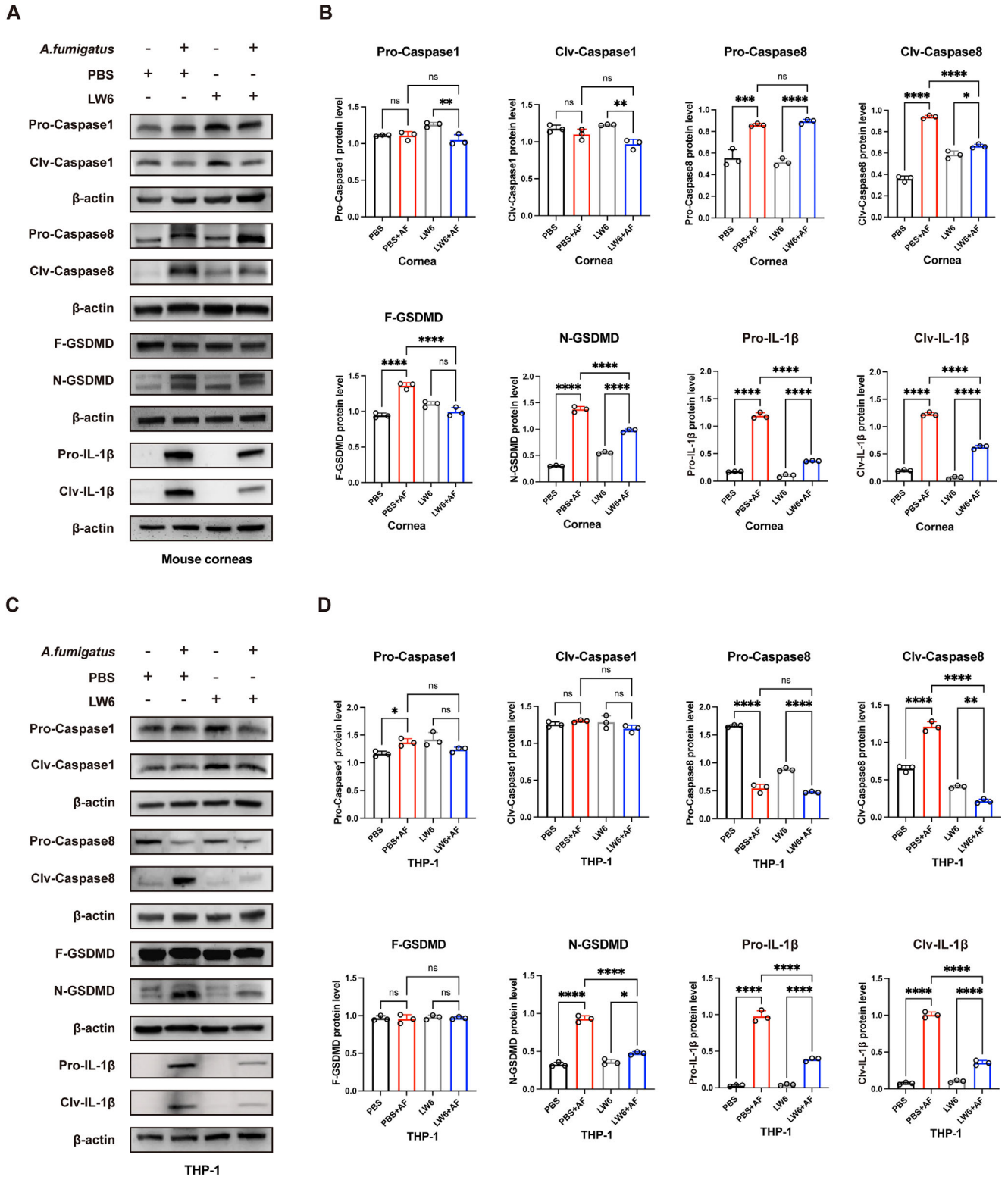

Figure 6. HIF-1α affects pyroptosis by regulating the caspase-8/GSDMD pathway. (**A**) Mouse corneas were treated with LW6 or control PBS before being inoculated with *A. fumigatus*. Corneal samples were obtained at 2 dpi for Western blot analysis of the protein expression levels of pro-caspase-1, clv-caspase-1, pro-caspase-8, clv-caspase-8, F-GSDMD, N-GSDMD, pro-IL-1β, and clv-IL-1β. (**B**) Grayscale analysis is shown in the bar graph. (**C**) THP-1 macrophages were treated with LW6 or control PBS and stimulated with *A. fumigatus*. Samples were collected at 16 hpi for Western blot analysis to detect the protein levels of pro-caspase-1, clv-caspase-1, pro-caspase-8, clv-caspase-8, F-GSDMD, N-GSDMD, pro-IL-1β, and clv-IL-1β. (**D**) Grayscale analysis is shown in the bar graph. The *P* values were generated using 1-way ANOVA, with ns = nonsignificant, $^{*}P < 0.05$, $^{**}P < 0.01$, $^{***}P < 0.001$, $^{****}P < 0.0001$. Data are presented as mean ± SEM from three different experiments with six mice per group.

lower inflammatory response in the inhibitor group may be linked to the downregulation of pyroptosis following HIF-1α inhibiting.

Discussion

The present study demonstrated that HIF-1α was markedly induced by *A. fumigatus* infection in C57BL/6 mice, THP-1 macrophages, and HCECs during the early stages of infection. Functional analysis revealed that the inhibition of HIF-1α resulted in faster epithelial repair, reduced inflammation response, infiltration of macrophages, and changed macrophage phenotypes during *A. fumigatus* infection. Additionally, the application of LW6 markedly reversed the elevated expression of pyroptotic proteins, specifically the caspase-8/GSDMD pathway. Collectively, our findings suggest that HIF-1α may be a key regulator in the immune response to fungal infections and increases corneal susceptibility to *A. fumigatus* infections.

The corneal epithelium is essential for immune defense. In the early phases of infection, most invasive pathogens remain within the epithelial layer.[27,28] Pathogens in the epithelium can be innately killed within the first few hours of infection, significantly reducing their invasion into the stroma.[29] Our study found that HIF-1α inhibited corneal epithelial repair, supporting the notion that epithelium is the primary site of innate defense. It suggests that the epithelial layer is probably where HIF-1α's effects on innate defense mechanisms begin, impairing mucosal immunity at the ocular surface.

After breaching the defenses of the corneal epithelium, the fungus invades the corneal stroma. In response to tissue infection, the host mounts an acute inflammatory response to contain the invasive pathogens.[30] The presence of *A. fumigatus* on the cornea triggers vasodilation in the adjacent tissues. This process facilitates the recruitment of macrophages and neutrophils. These immune cells subsequently release inflammatory mediators that not only mediate the inflammatory response but also initiate an immune response.[31–33] Our results clearly indicated that the inflammatory response of the cornea was reduced and the quantity of macrophages decreased in the cornea of mice following the inhibition of HIF-1α, confirming that HIF-1α can promote the recruitment of macrophages into the corneal stroma. CFU counting experiments confirmed that the ability of immune cells to phagocytose spores of *A. fumigatus* significantly decreased after inhibition with HIF-1α. In other studies, it has been found that HIF-1α performs a corresponding regulatory effect on local tissues by acting on macrophages and neutrophils.[34,35] Our research findings are similar, with the activity of HIF-1α being able to promote the recruitment and phagocytosis of macrophages to a certain extent, thereby facilitating the inflammatory response in keratitis.

The macrophage immune mechanism consists of two classical parts: activated M1 and M2 macrophages.[7,36,37] M1 macrophages are classically activated immune cells that play a crucial role in pro-inflammatory responses, leading to the production of key pro-inflammatory cytokines, including TNF-α and IL-6. In contrast, M2 macrophages are alternatively activated and are primarily involved in anti-inflammatory processes and tissue repair. One of the key cytokines produced by M2 macrophages is IL-10, which is a potent anti-inflammatory mediator. Reducing the recruitment of macrophages and promoting the M2 phenotype can help in reducing inflammation and promoting tissue repair, which is crucial for the cornea to reduce inflammation and restore transparency. The transition from M1 to M2 macrophage phenotypes holds substantial significance. These phenotypes respond distinctively to various immune challenges and play a crucial role in the pathogenesis of FK.[32,38] Consistent with this, our experimental findings demonstrated that LW6 pretreatment effectively suppressed the expression of M1-associated inflammatory factors, namely TNF-α and IL-6. Conversely, it enhanced the expression of M2-associated inflammatory factors, specifically IL-10. We plan to incorporate the ELISA detection method in future experiments, which can directly measure the secreted forms of cytokines and offers high sensitivity and specificity. Flow cytometry analysis more intuitively demonstrated that inhibiting HIF-1α led to a reduction in both the total macrophage cell rate and the M1 macrophage cell rate in mouse corneas. Meanwhile, the ratio of M2 to M1 macrophages was increased. Similarly, Eva et al.[39] demonstrated that inhibiting HIF-1α mitigated the LPS-induced pro-inflammatory M1 macrophage phenotype while promoting characteristics typical of the M2 macrophage phenotype. Wu et al.[40] demonstrated that targeted inhibition of HIF-1α effectively alleviated ulcerative colitis in mice. This therapeutic effect was likely achieved by suppressing the M1 macrophage phenotype while promoting the polarization of macrophages towards the M2 phenotype. By modulating HIF-1α activity, we may be able to influence the balance between these two phenotypes, which could have therapeutic implications in various inflammatory and immune-related diseases.

Infection and pyroptosis act as combined inflammatory triggers, playing critical roles in clearing microorganisms and healing host tissue damage during *A. fumigatus* infection.[25] The classical pathway of pyroptosis mainly relies on caspase 1, which can cleave the GSDMD protein. Interestingly, our research indicates that in FK, HIF-1α-mediated pyroptosis occurs through the caspase-8 pathway, rather than the classical pathway. A recent study on rheumatoid arthritis (RA) indicated that inhibiting HIF-1α can suppress hypoxia-induced pyroptosis in patients with RA.[41] Our findings regarding HIF-1α as a negative mediator in *A. fumigatus* keratitis are consistent with the RA study, albeit through distinct mechanisms. In our *A. fumigatus* keratitis model, HIF-1α induces the caspase-8/GSDMD signaling pathway, promoting the release of the downstream factor IL-1β, which results in a stronger inflammatory response. Based on these results, the inflammatory response mediated by HIF-1α in our study is a complex process involving both epithelial and immune components. The corneal epithelial cells play a key role in initiating the response and wound healing, but the immune cells such as macrophages also contributes to the overall inflammatory outcome.

Using LW6 alone to examine HIF-1α's role is a study limitation. Future research should use genetic knockdown methods like siRNA or CRISPR to validate effects and better understand HIF-1α.

Conclusions

In summary, our findings demonstrated that HIF-1α might play a critical pro-inflammatory role in *A. fumigatus* keratitis by activating pyroptosis through caspase-8/ GSDMD pathway. These conclusions are supported by data from a diverse range of experimental models, including *A. fumi-*

Investigative Ophthalmology & Visual Science

gatus keratitis in mice, THP-1 macrophages, and human corneal epithelial cell lines.

Acknowledgments

Supported by the National Natural Science Foundation of China (No. 82171019), Natural Science Foundation of Shandong Province (No. ZR2021MH368), the Medical Science and Technology Key Project of Shandong (No. 202307021598), and the Special Funding for Qilu Sanitation and Health Leading Talents Cultivation Project.

Disclosure: **H. Yang**, None; **M. Liu**, None; **S. Song**, None; **Q. Xu**, None; **J. Lee**, None; **J. Sun**, None; **S. Xue**, None; **X. Sun**, None; **C. Che**, None

References

1. Hoffman JJ, Burton MJ, Leck A. Mycotic keratitis-a global threat from the filamentous fungi. *J Fungi (Basel)*. 2021;7.
2. Manikandan P, Abdel-Hadi A, Randhir Babu Singh Y, et al. Fungal keratitis: epidemiology, rapid detection, and antifungal susceptibilities of fusarium and aspergillus isolates from corneal scrapings. *Biomed Res Int*. 2019;2019: 6395840.
3. Bhartiya P, Daniell M, Constantinou M, Islam FM, Taylor HR. Fungal keratitis in Melbourne. *Clin Exp Ophthalmol*. 2007;35:124–130.
4. Mascarenhas M, Chaudhari P, Lewis SA. Natamycin ocular delivery: challenges and advancements in ocular therapeutics. *Adv Ther*. 2023;40:3332–3359.
5. Medzhitov R. Origin and physiological roles of inflammation. *Nature*. 2008;454:428–435.
6. Ross BX, Gao N, Cui X, Standiford TJ, Xu J, Yu FX. IL-24 promotes pseudomonas aeruginosa keratitis in C57BL/6 mouse corneas. *J Immunol*. 2017;198:3536–3547.
7. Akira S, Uematsu S, Takeuchi O. Pathogen recognition and innate immunity. *Cell*. 2006;124:783–801.
8. Constant DA, Nice TJ, Rauch I. Innate immune sensing by epithelial barriers. *Curr Opin Immunol*. 2021;73:1–8.
9. Zhao GQ, Hu M, Li C, et al. Osteopontin contributes to effective neutrophil recruitment, IL-1β production and apoptosis in keratitis. *Immunol Cell Biol*. 2018;96:401–412.
10. Yang H, Wang Q, Han L, et al. Nerolidol inhibits the LOX-1 /IL-1beta signaling to protect against the Aspergillus fumigatus keratitis inflammation damage to the cornea. *Int Immunopharmacol*. 2020;80:106118.
11. Niethammer P, Grabher C, Look AT, Mitchison TJ. A tissue-scale gradient of hydrogen peroxide mediates rapid wound detection in zebrafish. *Nature*. 2009;459:996–999.
12. Katikaneni A, Jelcic M, Gerlach GF, Ma Y, Overholtzer M, Niethammer P. Lipid peroxidation regulates long-range wound detection through 5-lipoxygenase in zebrafish. *Nat Cell Biol*. 2020;22:1049–1055.
13. Uderhardt S, Martins AJ, Tsang JS, Lammermann T, Germain RN. Resident macrophages cloak tissue microlesions to prevent neutrophil-driven inflammatory damage. *Cell*. 2019;177:541–555.e517.
14. Razzell W, Evans IR, Martin P, Wood W. Calcium flashes orchestrate the wound inflammatory response through DUOX activation and hydrogen peroxide release. *Curr Biol*. 2013;23:424–429.
15. Iyer NV, Kotch LE, Agani F, et al. Cellular and developmental control of O2 homeostasis by hypoxia-inducible factor 1 alpha. *Genes Dev*. 1998;12:149–162.
16. McGettrick AF, O'Neill LAJ. The role of HIF in immunity and inflammation. *Cell Metab*. 2020;32:524–536.
17. Lee JW, Bae SH, Jeong JW, Kim SH, Kim KW. Hypoxia-inducible factor (HIF-1)alpha: its protein stability and biological functions. *Exp Mol Med*. 2004;36:1–12.
18. Alonso D, Serrano E, Bermejo FJ, Corral RS. HIF-1alpha-regulated MIF activation and Nox2-dependent ROS generation promote Leishmania amazonensis killing by macrophages under hypoxia. *Cell Immunol*. 2019;335:15–21.
19. Baay-Guzman GJ, Duran-Padilla MA, Rangel-Santiago J, et al. Dual role of hypoxia-inducible factor 1 alpha in experimental pulmonary tuberculosis: its implication as a new therapeutic target. *Future Microbiol*. 2018;13:785–798.
20. Niu Y, Zhao G, Li C, et al. Aspergillus fumigatus increased PAR-2 expression and elevated proinflammatory cytokines expression through the pathway of PAR-2/ERK1/2 in cornea. *Invest Ophthalmol Vis Sci*. 2018;59:166–175.
21. Wu TG, Wilhelmus KR, Mitchell BM. Experimental keratomycosis in a mouse model. *Invest Ophthalmol Vis Sci*. 2003;44:210–216.
22. Jiang N, Zhang L, Zhao G, et al. Indoleamine 2,3-dioxygenase regulates macrophage recruitment, polarization and phagocytosis in Aspergillus fumigatus keratitis. *Invest Ophthalmol Vis Sci*. 2020;61:28.
23. Guibo L, Chunxu D, Biao C, et al. Dectin-1 participates in the immune-inflammatory response to mouse Aspergillus fumigatus keratitis by modulating macrophage polarization. *Front Immunol*. 2024;15:1431633.
24. Liu S, Hur YH, Cai X, et al. A tissue injury sensing and repair pathway distinct from host pathogen defense. *Cell*. 2023;186:2127–2143.e2122.
25. Zhao W, Yang H, Lyu L, et al. GSDMD, an executor of pyroptosis, is involved in IL-1beta secretion in Aspergillus fumigatus keratitis. *Exp Eye Res*. 2021;202:108375.
26. Bedoui S, Herold MJ, Strasser A. Emerging connectivity of programmed cell death pathways and its physiological implications. *Nat Rev Mol Cell Biol*. 2020;21:678–695.
27. Yoon GS, Dong C, Gao N, Kumar A, Standiford TJ, Yu FS. Interferon regulatory factor-1 in flagellin-induced reprogramming: potential protective role of CXCL10 in cornea innate defense against Pseudomonas aeruginosa infection. *Invest Ophthalmol Vis Sci*. 2013;54:7510–7521.
28. Liu X, Gao N, Dong C, et al. Flagellin-induced expression of CXCL10 mediates direct fungal killing and recruitment of NK cells to the cornea in response to Candida albicans infection. *Eur J Immunol*. 2014;44:2667–2679.
29. Evans DJ, Fleiszig SM. Why does the healthy cornea resist Pseudomonas aeruginosa infection? *Am J Ophthalmol*. 2013;155:961–970.e962.
30. Basil MC, Levy BD. Specialized pro-resolving mediators: endogenous regulators of infection and inflammation. *Nat Rev Immunol*. 2016;16:51–67.
31. Yang J, Yin S, Bi F, et al. TIMAP repression by TGFbeta and HDAC3-associated Smad signaling regulates macrophage M2 phenotypic phagocytosis. *J Mol Med (Berl)*. 2017;95:273–285.
32. Hu J, Wang Y, Xie L. Potential role of macrophages in experimental keratomycosis. *Invest Ophthalmol Vis Sci*. 2009;50:2087–2094.
33. Brown BN, Ratner BD, Goodman SB, Amar S, Badylak SF. Macrophage polarization: an opportunity for improved outcomes in biomaterials and regenerative medicine. *Biomaterials*. 2012;33:3792–3802.
34. Wang Y, Zhang M, Bi R, et al. ACSL4 deficiency confers protection against ferroptosis-mediated acute kidney injury. *Redox Biol*. 2022;51:102262.
35. Nakamura A, Jo S, Nakamura S, et al. HIF-1alpha and MIF enhance neutrophil-driven type 3 immunity and chondrogenesis in a murine spondyloarthritis model. *Cell Mol Immunol*. 2024;21:770–786.

36. Lopes RL, Borges TJ, Zanin RF, Bonorino C. IL-10 is required for polarization of macrophages to M2-like phenotype by mycobacterial DnaK (heat shock protein 70). *Cytokine*. 2016;85:123–129.
37. Xia T, Fu S, Yang R, et al. Advances in the study of macrophage polarization in inflammatory immune skin diseases. *J Inflamm (Lond)* . 2023;20:33.
38. Barros MH, Hauck F, Dreyer JH, Kempkes B, Niedobitek G. Macrophage polarisation: an immunohistochemical approach for identifying M1 and M2 macrophages. *PLoS One*. 2013;8:e80908.
39. Palsson-McDermott EM, Curtis AM, Goel G, et al. Pyruvate kinase M2 regulates Hif-1alpha activity and IL-1beta induction and is a critical determinant of the Warburg effect in LPS-activated macrophages. *Cell Metab*. 2015;21:65–80.
40. Wu MM, Wang QM, Huang BY, et al. Dioscin ameliorates murine ulcerative colitis by regulating macrophage polarization. *Pharmacol Res*. 2021;172:105796.
41. Hong Z, Wang H, Zhang T, et al. The HIF-1/BNIP3 pathway mediates mitophagy to inhibit the pyroptosis of fibroblast-like synoviocytes in rheumatoid arthritis. *Int Immunopharmacol*. 2024;127:111378.

Investigative Ophthalmology & Visual Science